



Missouri University of Science and Technology
Scholars' Mine

Physics Faculty Research & Creative Works

Physics

01 Apr 1968


Associative Detachment: $H+H^{-} \rightarrow 2^{*} + e$

Joseph C.Y. Chen

Jerry Peacher

Missouri University of Science and Technology, peacher@mst.edu

Follow this and additional works at: https://scholarsmine.mst.edu/phys_facwork

 Part of the [Physics Commons](#)

Recommended Citation

J. C. Chen and J. Peacher, "Associative Detachment: $H+H^{-} \rightarrow 2^{*} + e$," *Physical Review*, vol. 168, no. 1, pp. 56-63, American Physical Society (APS), Apr 1968.

The definitive version is available at <https://doi.org/10.1103/PhysRev.168.56>

This Article - Journal is brought to you for free and open access by Scholars' Mine. It has been accepted for inclusion in Physics Faculty Research & Creative Works by an authorized administrator of Scholars' Mine. This work is protected by U. S. Copyright Law. Unauthorized use including reproduction for redistribution requires the permission of the copyright holder. For more information, please contact scholarsmine@mst.edu.

Associative Detachment: $\text{H} + \text{H}^- \rightarrow \text{H}_2^* + e^\dagger$

JOSEPH C. Y. CHEN AND JERRY L. PEACHER*

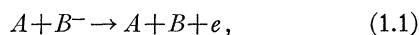
*Department of Physics and Institute for Pure and Applied Physical Sciences,
University of California, San Diego, La Jolla, California*

(Received 1 November 1967)

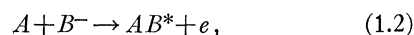
The process of associative detachment in the (H, H^-) collision system is investigated at energies below 12 eV. In this energy region, the interaction potential between H and H^- has recently been determined. The energy dependence of the cross section is calculated with explicit allowance for the production of "hot" hydrogen molecules. It is observed that associative detachment provides a possible mechanism for generating an inverted population of the residual molecule such as H_2 .

I. INTRODUCTION

DURING the collision encounter between an atom A and an ion B^- , electron detachment may occur, leading to the processes of collisional detachment

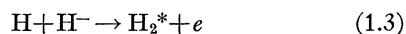


and associative detachment



where the asterisk indicates that AB may be internally excited. The detachment potential of B^- (or the negative of the electron affinity of B) gives rise to a threshold for the collisional-detachment process. Since the detachment potential of most systems of interest such as H^- , O^- , and O_2^- is usually large (from a few electron volts down to a few tenths) in comparison with the mean kinetic energy of the ionized gases at moderate temperatures, this process is therefore not expected to be very important in ionized gases at temperatures, say, less than a few thousand degrees Kelvin. On the other hand, the energy released in forming bound states of the AB^* molecule in the associative detachment is sufficient to overtake the detachment potential. Associative-detachment processes are therefore exothermic. Consequently, the latter process [Eq. (1.2)] may be of importance in ionized gases at temperatures down to a few hundred degrees or less since at such low temperatures associative detachment provides the only mechanism for electron detachment from negative ions by collisions without the participation of metastable species or photons.

It was suggested by Dalgarno¹ that associative detachment of electrons from hydrogen ions by collision with atomic hydrogen



may constitute, in comparison with photodetachment, an efficient mechanism for the electron detachment of H^- ions in the solar photosphere. The rate coefficient

[†] This research was supported by the Advanced Research Projects Agency (Project DEFENDER) and was monitored by the U. S. Army Research Office (Durham) under Contract No. DA-31-124-ARO-D-257.

* Present address: Space Science Laboratory, University of California, Berkeley, Calif.

¹ Quoted in the paper by B. E. J. Pagel, *Hon. Hot. R. Astron. Soc.* **119**, 609 (1959); and private communication.

for such an associative-detachment process is estimated to be of the order of $10^{-9} \text{ cm}^3 \text{ sec}^{-1}$. A calculation of the rate coefficient using the recent complex potential curves for H_2^- ion has been carried out elsewhere.² The purpose of the present paper is not to calculate the rate coefficient but rather to study the details of the cross section for the production of H_2 in various vibrational and rotational states in associative detachment over a significant energy range, including the very low-energy region. We will confine our study to the case where both H and H^- are initially in their ground states. A brief account of this work was presented recently at the Leningrad conference.³ Collisional detachment for the (H, H^-) system will be considered elsewhere.

Our approach to the problem is based on the theory of atomic collisions with negative ions recently formulated by one of us.⁴ The basic physical picture upon which the theory is formulated can be summarized as follows: For a given set of initial states of atom A and ion B^- , there exists a real interaction potential for A and B^- at large internuclear separation R . This interaction potential splits into several components (according to the net resultant angular momentum along the internuclear axis, spin multiplicities, etc.) due to a strong local electric field created along the internuclear axis as A and B^- approach each other with their electronic states gradually merging into that of the negative molecular ion AB^- . There is a correspondence between the components of the interaction potential and the electronic states of the AB^- ion. Along each component of the interaction potential there may exist a region of internuclear separation within which the interaction potential along this component is complex, resulting from the fact that the corresponding electronic state of AB^- is unstable with respect to electron emission. Such a region where the potential is complex is characteristic of the system and of the electronic state which corresponds to the particular component of the potential in question. As A and B^- approach into these complex potential regions, electron emission may result and cause the interaction system (A, B^-) to decay into some

² A. Dalgarno and J. C. Browne, *Astrophys. J.* **149**, 231 (1967).

³ J. C. Y. Chen and J. L. Peacher, in *Proceedings of the Fifth International Conference on the Physics of Electronic and Atomic Collision* (Publishing House "Nauka," Leningrad, USSR, 1967), p. 335.

⁴ J. C. Y. Chen, *Phys. Rev.* **156**, 12 (1967).

molecular states of the AB molecule lying below, giving rise to the process of associative detachment.

For the (H, H^-) system of interest here with both H and H^- in their ground state, the interaction potential for H and H^- asymptotically lies below that for two ground-state H atoms by an amount corresponding to the electron affinity of H (0.755 eV). At smaller internuclear separations, the interaction potential splits into the *ungerade* and *gerade* modes, corresponding to the ${}^2\Sigma_u^+$ and ${}^2\Sigma_g^+$ H_2^- states, respectively. The two modes of interaction cross the potential curve of the ground ${}^1\Sigma_g^+$ state of the H_2 molecule with a continuum electron. Thus when H and H^- come closer than the crossing internuclear separation in the ungerade (or gerade) mode, the interaction potential becomes complex due to configuration interaction with the $H_2 + e$ continuum. This leads to electron emission and the decay of the interaction system (H, H^-) into some bound state of H_2 lying below, giving rise to the process of associative detachment.

Recently the complex interaction potential for H and H^- in both the ungerade and gerade modes were determined.^{5,6} Utilizing this interaction potential, the cross section for total detachment in each partial wave can be easily calculated by solving the nuclear Schrödinger equation for the imaginary parts of the nuclear phase shift $\zeta_J^{(u)}$ and $\zeta_J^{(g)}$ in the ungerade and gerade modes, respectively. The total cross section for electron detachment in each mode, irrespective of the final state of the nuclei, is

$$\sigma_D^{(u, g)} = \sum_J \sigma_J^{(u, g)} = \frac{\pi}{\kappa^2} \sum_J (2J+1) \{1 - |P_J^{(u, g)}|^2\}, \quad (1.4)$$

with

$$P_J^{(u, g)} = \exp\{-2\zeta_J^{(u, g)}\}, \quad (1.5)$$

where κ is the relative wave number of H and H^- and P_J is the survival probability against detachment of the electron during the collision encounter. Since for the (H, H^-) system of interest the two modes of interaction do not cross each other, the over-all total electron-detachment cross section is simply the algebraic sum of contributions coming from both modes of interaction,

$$\sigma_{\text{tot}} = \sigma_D^{(u)} + \sigma_D^{(g)}. \quad (1.6)$$

It is clear from Eq. (1.4) that, if the imaginary parts of the interaction are switched off, the survival probability becomes unity (since $\zeta_J^{(u, g)}$ becomes zero) and the electron-detachment cross section becomes zero. The detachment cross section is also bounded for each partial wave by the geometric cross section, i.e.,

$$\sigma_J^{(u, g)} < (2J+1)\pi/\kappa^2. \quad (1.7)$$

The maximum geometric cross section can be reached if the imaginary phase shift becomes very large (approaches infinity) so that the survival probability becomes essentially zero.

To calculate specifically the cross section for associative detachment the matrix elements between the scattering and associative-detachment channels must be evaluated explicitly. One then encounters the cumbersome electronic matrix elements which cannot be simply evaluated with desired accuracy. Since the imaginary interaction potential is related to the electronic matrix elements, an estimation of the electronic matrix elements can be made from the known values of the imaginary potential. In the present work, however, we elect to determine the electronic matrix elements semi-empirically from the measured cross section for dissociative attachment, the reverse process of associative detachment.

After a brief review of the expression for the cross section of associative detachment and some qualitative features of the complex interaction potential, the semi-empirical procedure for the determination of the electronic matrix elements is outlined in Sec. II. Calculation of these matrix elements is carried out in Sec. III in which the measured cross section for dissociative attachment is utilized.^{7,8} Having determined the electronic matrix elements, the associative-detachment cross section for the production of a stable molecule in some specified rotational and vibrational state is then calculated. The results are presented in graphic form. Finally, in Sec. IV some concluding remarks are given.

II. THEORETICAL CONSIDERATION

A. Expression for the Cross Section

The total cross section for associative detachment is a sum of the partial cross sections for the production of the residual molecule in specific sets of vibrational and rotational states (vL) resulting from electron detachment.

$$\sigma_{\text{tot}}^{AD} = \sum_{vL} \sigma_{vL}^{AD}. \quad (2.1)$$

The partial cross section σ_{vL}^{AD} consists of a sum over each partial wave J of H and H^- and a sum over each partial wave l of the detached electron. Since the total angular momentum of the reaction system must be conserved, we have the selection rule⁹

$$|L-l| \leq J \leq L+l. \quad (2.2)$$

We now write

$$\sigma_{vL}^{AD} = \sum_l \sigma_{lvL}^{AD}, \quad (2.3)$$

where the l sum is left unrestricted and the sum over J in obtaining σ_{lvL}^{AD} has been carried out in accordance

⁵ J. C. Y. Chen and J. L. Peacher, Phys. Rev. **167**, 30 (1968).

⁶ J. N. Bardsley, A. Herzenberg, and F. Mandl, Proc. Phys. Soc. (London) **89**, 305 (1966).

⁷ D. Rapp, T. E. Sharp, and D. D. Briglia, Phys. Rev. Letters **14**, 533 (1965).

⁸ G. J. Schulz and R. K. Asundi, Phys. Rev. **158**, 25 (1967).

⁹ J. C. Y. Chen and J. L. Peacher, Phys. Rev. **163**, 103 (1967).

with the selection rule [Eq. (2.2)]. This allows us to examine the distribution of σ_{vL}^{AD} in terms of the partial wave l of the detached electron.

The partial cross section for electron detachment into the partial wave l in the case of H and H⁻ is

$$\sigma_{lvL}^{AD} = \frac{1}{4}\sigma_{AD}^{(1)}(lv, \text{even}L) + \frac{3}{4}\sigma_{AD}^{(3)}(lv, \text{odd}L), \quad (2.4)$$

where the superscripts (1) and (3) denote the spin multiplicities of the nuclei and the coefficients $\frac{1}{4}$ and $\frac{3}{4}$ are the statistical weights. Assuming that the electronic matrix elements are slowly varying functions of the internuclear separation so that their dominant contributions come at the equilibrium internuclear separation R_e of the ground ${}^1\Sigma_g^+$ state of H₂, the cross section may be written as⁹

$$\sigma_{AD}^{(1,3)}(lv, L) = \frac{k_i}{\kappa} \beta_l^{(u,g)}(R_e) G_{lvL}(u, g \rightarrow g), \quad (2.5)$$

where $\beta_l^{(u)}$ and $\beta_l^{(g)}$ are related to the absolute square of the electronic matrix elements for associative detachment resulting from the ungerade and gerade modes of interaction, respectively. The weak dependence of the β 's on the vibrational states of H₂ is suppressed. The G_{lvL} functions are restricted sums over nuclear overlap integrals (between the continuum nuclear wave function of H and H⁻ and the vibrational nuclear wave function of H₂) with appropriate coefficients for each contributing J partial wave.

Symmetry consideration with respect to interchange of nuclei in the homonuclear case such as H₂ and D₂ leads to a further constraint in parity matching between L and J . For associative detachment resulting from the ungerade mode of interaction, the participating nuclear states J and L must have opposite parity; for the gerade mode of interaction, on the other hand, J and L have the same parity. This further restricts the J sum in the G_{lvL} functions. Thus for the detachment of an s -wave ($l=0$) electron,⁹ we have

$$\begin{aligned} G_{0vL}(u \rightarrow g) &= 0, \\ G_{0vL}(g \rightarrow g) &= \mu |\langle \chi_v | \xi_L^{(g)} \rangle|^2 e^{-2\zeta_L^{(g)}}, \end{aligned} \quad (2.6)$$

and for a p wave ($l=1$) electron

$$\begin{aligned} G_{1vL}(u \rightarrow g) &= \mu C_{L+1} |\langle \chi_v | \xi_{L+1}^{(u)} \rangle|^2 e^{-2\zeta_{L+1}^{(u)}} \\ &\quad + \mu C_{L-1} |\langle \chi_v | \xi_{L-1}^{(u)} \rangle|^2 e^{-2\zeta_{L-1}^{(u)}}, \end{aligned} \quad (2.7)$$

$G_{1vL}(g \rightarrow g) = 0$, etc.,

where μ is the reduced mass, the χ_v 's and ξ 's are the vibrational and continuum nuclear wave functions respectively, and the ζ 's are the imaginary parts of the nuclear phase shift. The $C_{L\pm 1}$ are related to the Clebsch-Gordan coefficient

$$C_{L\pm 1} = [2(L\pm 1) + 1] \begin{pmatrix} L\pm 1 & 1 & L \\ 0 & 0 & 0 \end{pmatrix}^2. \quad (2.8)$$

B. Damped Continuum Wave Function

The continuum nuclear radial wave functions ξ_J are solutions of the equations (in atomic units)

$$\left\{ \frac{d^2}{dr^2} + \frac{J(J+1)}{R^2} + 2\mu[E - V_{u,g}(R) + \frac{1}{2}i\Gamma_{u,g}(R)] \right\} \times \xi_J^{(u,g)}(R) = 0, \quad (2.9)$$

where the complex potentials $V_u - \frac{1}{2}i\Gamma_u$ and $V_g - \frac{1}{2}i\Gamma_g$ for the ungerade and gerade modes of interaction between H and H⁻ are represented by the lowest ${}^2\Sigma_u^+$ and ${}^2\Sigma_g^+$ states of H₂⁻, respectively. Because of the presence of the imaginary interaction, the $\xi_J^{(u,g)}$'s are damped waves resulting from electron emission.

We solve Eq. (2.9) by the JWKB approximation. The proper solution for ξ at the right-hand side of the turning point R_0 is

$$\begin{aligned} \xi_J(R) &= NK_J(R)^{-1/2} \\ &\times \sin \left\{ \frac{1}{4}\pi + [\alpha_J \Gamma(R_0)]^{3/2} + \int_{R_0}^R K_J(R') dR' \right\}, \end{aligned} \quad (2.10)$$

and at the left-hand side of the turning point

$$\begin{aligned} \xi_J(R) &= \frac{1}{2}NK_J(R)^{-1/2} \\ &\times \exp \left\{ -[\alpha_J \Gamma(R_0)]^{3/2} - \int_R^{R_0} K_J(R') dR' \right\}, \end{aligned} \quad (2.11)$$

with

$$K_J(R) = \{2\mu[E - u_J(R) + i\frac{1}{2}\Gamma(R)]\}^{1/2}, \quad (2.12)$$

$$u_J(R) = V(R) + (J + \frac{1}{2})^2 / (2\mu R^2), \quad (2.13)$$

$$\alpha_J(R_0) = i \left\{ \frac{1}{9}\mu \left/ \left[\frac{1}{2}i \frac{d\Gamma(R)}{dR} - \frac{du_J(R)}{dR} \right]^2 \right. \right\}^{1/3}_{R=R_0}, \quad (2.14)$$

where N is a normalization constant, and where α_J arises from the imaginary part of the potential in matching with the Airy-function solution at the turning point R_0 .

Examining Eq. (2.10), it is clear that $\xi_J(R)$ satisfies the usual asymptotic expression

$$\xi_J(R) \xrightarrow{R \rightarrow \infty} \kappa^{-1} (\sin \kappa R - \frac{1}{2}J\pi + \eta_J), \quad (2.15)$$

where

$$\eta_J = \delta_J + i\zeta_J \quad (2.16)$$

is the complex phase shift. Because of this imaginary part of the phase shift, the asymptotic amplitude of oscillation for either the real or imaginary part of ξ_J is proportional to the exponential of ζ_J , i.e., $\exp(\zeta_J)$. This can be seen by writing Eq. (2.15) as

$$\text{Re}\{\xi_J(R)\} \xrightarrow{R \rightarrow \infty} \kappa^{-1} \cosh \zeta_J \sin(\kappa R - \frac{1}{2}J\pi + \delta_J), \quad (2.17)$$

$$\text{Im}\{\xi_J(R)\} \xrightarrow{R \rightarrow \infty} \kappa^{-1} \sinh \zeta_J \cos(\kappa R - \frac{1}{2}J\pi + \delta_J). \quad (2.18)$$

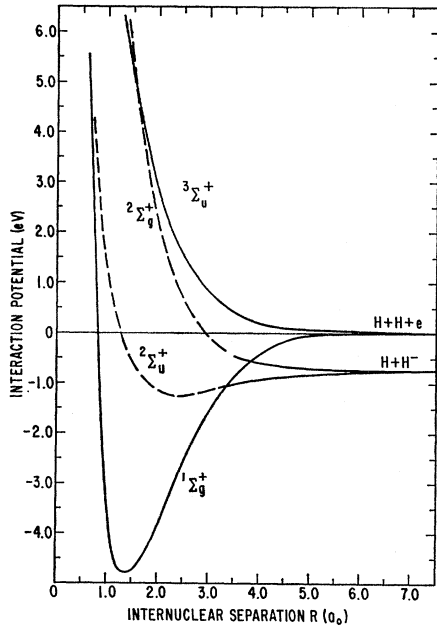


FIG. 1. The real parts $V_u(R)$ and $V_g(R)$ of the interaction potential between the ground states of H and H^- together with the potential curves of the residual H_2 molecule with an asymptotic continuum electron. The curves are obtained from Refs. 10 and 11, respectively.

Numerically it is therefore more convenient to incorporate the survival probability factor $\exp(-2\zeta_J)$ [see Eqs. (2.7) and (2.8)] into ξ_J .

C. Complex Interaction Potential

The complex interaction potential for H and H^- in both the ungerade and gerade modes were recently determined semiempirically by us.⁵ A comparison of the result with previous calculations⁶ was also discussed there. This potential is given by the following expressions:

$$V_u(R) = 0.5 \{ \exp\{-1.7773(R-2.33)\} - 2 \exp\{-0.88865(R-2.33)\} \}, \quad (2.19)$$

$$\Gamma_u(R) = 3.08 \exp\{-0.386(R-0.9)^2\}, \quad (2.20)$$

$$V_g(R) = 57 \exp\{-1.4886R\}, \quad (2.21)$$

$$\Gamma_g(R) = 1.16 \exp\{-0.28(R-1.2)^2\}, \quad (2.22)$$

where both the V 's and Γ 's are in units of electron volts and R is in units of the Bohr radius a_0 . A plot of the potential is given in Figs. 1 and 2. For the purpose of discussion the lowest $^1\Sigma_g^+$ and $^3\Sigma_u^+$ states of the H_2 molecule¹⁰ are also included in Fig. 1.

Utilizing the complex interaction, the continuum radial wave function $\xi_J(R)$ can be easily calculated. The cross section for associative detachment can then be evaluated if the electronic factor $B_l^{(u,\theta)}$ is known. As mentioned in the Introduction, we proposed to deduce the β 's from the measured cross section for dis-

¹⁰ W. Kolos and L. Wolnicwicz, J. Chem. Phys. 43, 2429 (1965).

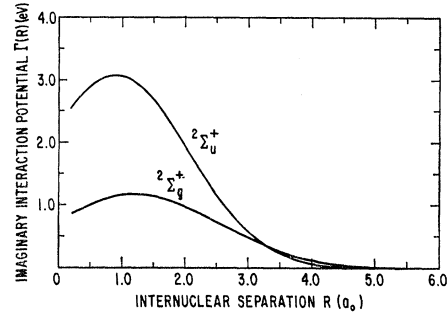


FIG. 2. The imaginary parts $\Gamma_u(R)$ and $\Gamma_g(R)$ of the interaction potential between the ground states of H and H^- obtained from Ref. 10.

sociative attachment in the (e, H_2) system. It should be noted that in the $g \rightarrow g$ dissociative-attachment cross section, some structure around an incident electron energy of about 10 eV was observed by Schulz.¹¹ Recent measurements by Rapp *et al.*⁷ with higher resolution does not reproduce the previously observed dip in the (e, H_2) case. Such a dip was nevertheless observed by Rapp *et al.*⁷ for dissociative attachment in the (e, HD) and (e, D_2) isotope systems. Since the gerade mode of the complex potential adopted here for the $g \rightarrow g$ interaction is a phenomenological potential,⁵ we do not expect it to account for the observed structure.

We choose to deduce the electronic factor $\beta_l^{(\theta)}$ from the dissociative-attachment cross section for the (e, H_2) system measured by Rapp *et al.*⁷ Consequently the details of this structure will not be considered explicitly. We note that further structures have been observed in the $g \rightarrow g$ dissociative-attachment cross section above about 11 eV of the incident electron.¹² This may be due to the coupling of the $^2\Sigma_g^+ + H_2^-$ state with a closed-channel resonant state of H_2^- . Such a mechanism has been discussed elsewhere.¹³ We will not consider these structures in the present investigation.

D. Electronic Matrix Element

The square of the electronic matrix elements $\beta_l^{(u)}$ and $\beta_l^{(\theta)}$ can be determined semiempirically by matching the theoretical cross section with the observed cross section for dissociative attachment. The thermal averaged dissociative-attachment cross section with an appropriate allowance for the energy distribution of the experimental electron beam is given for the (e, H_2) system by

$$\bar{\sigma}_{DA}(\bar{E}, T) = \int D(E, \bar{E}) \bar{\sigma}_{DA}^{(u,\theta)}(E, T) dE, \quad (2.23)$$

with

$$\bar{\sigma}_{DA}^{(u,\theta)}(E, T) = \frac{\beta_l^{(u,\theta)}}{Zk_i} \sum_v \left\{ \sum_{\text{even } L} + 3 \sum_{\text{odd } L} \right\} 2\kappa_{vL} (2L+1) \times G_{lvL}(g \rightarrow u, g) \exp\{-(\epsilon_v + \epsilon_L)/KT\}, \quad (2.24)$$

¹¹ G. J. Schulz, Phys. Rev. 113, 816 (1959).

¹² J. T. Dowell and T. E. Sharp (to be published).

¹³ See Sec. IV.2 in Ref. 4.

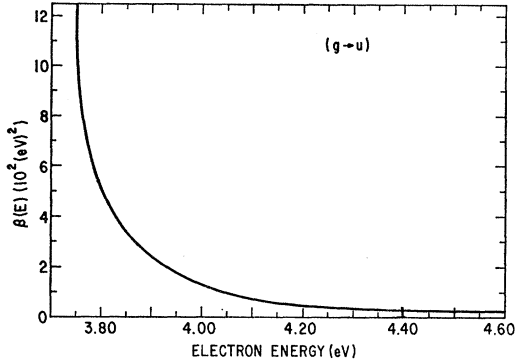


FIG. 3. The electronic factor $\beta_1(E)$ (which is related to the absolute square of the electronic matrix element) for the transition between the ${}^1\Sigma_g^+$ H_2 state with a continuum electron and the ${}^2\Sigma_u^+$ H_2^- state deduced semiempirically from the $g \rightarrow u$ dissociative-attachment cross section in the (e, H_2) system as observed by Schulz and Asundi (Ref. 8).

where Z^{-1} is the partition function of the H_2 molecule, k_z and κ_{vL} are the wave numbers of the incident electron and dissociating H and H^- , and $D(E, \bar{E})$ is the energy distribution function of the electron beam.

The expression for $\bar{\sigma}_{DA}^{(u, \vartheta)}$ given by Eq. (2.24) is valid for a given partial wave l of the incident electron. In order to compare the theoretical cross section given by Eq. (2.23) with measurements, one must sum $\bar{\sigma}_{DA}^{(u, \vartheta)}$ over all the contributing partial waves of the incident electron. This then makes the determination of the β 's very difficult. We approximate Eq. (2.24) by taking $l=1$ and 0 and then define an averaged electronic factor $\beta_1^{(u)}$ and $\beta_0^{(\vartheta)}$ for the ungerade and gerade cases, respectively. This is basically a lowest-partial-wave approximation which should be good at low incident-electron energy since the leading waves are p and s waves for the $g \rightarrow u$ and $g \rightarrow g$ dissociative attachment, respectively. Deviations from this approximation will then appear in the semiempirical $\beta_1^{(u)}$ and $\beta_0^{(\vartheta)}$.

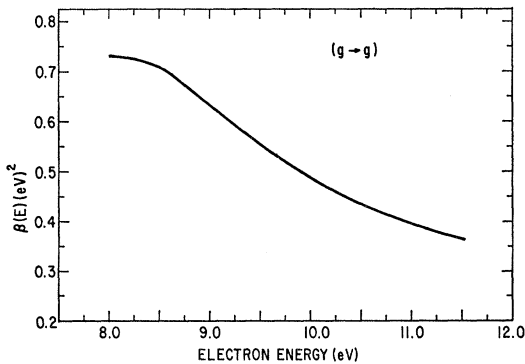


FIG. 4. The electronic factor $\beta_0(E)$ (which is related to the absolute square of the electronic matrix element) for the transition between the ${}^1\Sigma_g^+$ H_2 state with a continuum electron and the ${}^2\Sigma_g^+$ H_2^- state deduced semiempirically from the $g \rightarrow g$ dissociative-attachment cross section in the (e, H_2) system observed by Rapp *et al.* (Ref. 7).

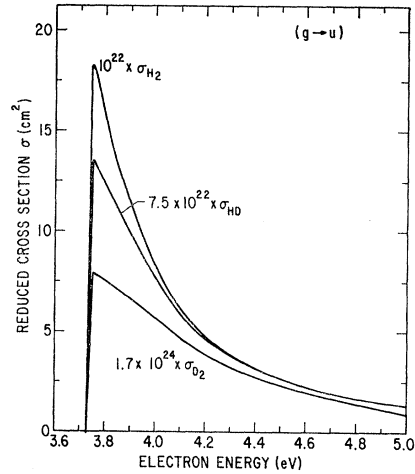


FIG. 5. The reduced cross section for the $g \rightarrow u$ dissociative attachment in the (e, H_2) system obtained by unfolding the measured cross section of Schulz and Asundi (Ref. 8) with a beam width of 0.1 eV. The curves labelled HD and D_2 are the calculated dissociative-attachment cross section using the semiempirical β_1 (Fig. 3) deduced from the (e, H_2) system.

III. RESULTS AND DISCUSSION

The electronic factors $\beta_1^{(u)}$ and $\beta_0^{(\vartheta)}$ are obtained by fitting the theoretical cross section $\bar{\sigma}_{DA}^{(u, \vartheta)}(\bar{E}, T)$ with the observed cross section of the (e, H_2) system at room temperature $T=300^\circ\text{K}$ with appropriate distribution functions $D(E, \bar{E})$ which characterize the electron beams used by Schulz and Asundi⁸ and by Rapp *et al.*⁷ for the $g \rightarrow u$ and $g \rightarrow g$ dissociative attachments, respectively (see Appendix). The electronic matrix elements so

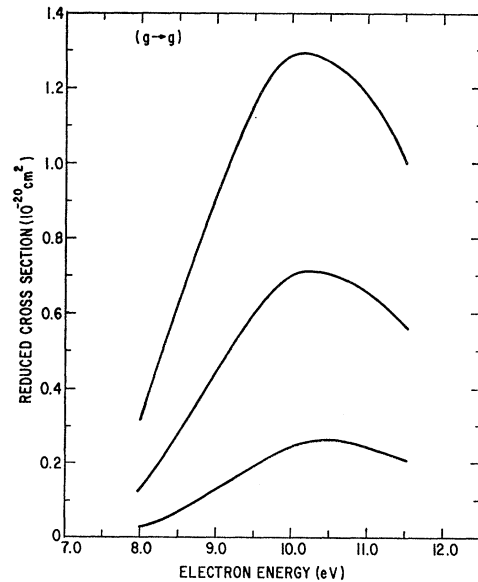


FIG. 6. The reduced cross section for the $g \rightarrow g$ dissociative attachment in the (e, H_2) system obtained by unfolding the measured cross section of Rapp *et al.* (Ref. 8) with a beam width of 0.3 eV. The curves labelled HD and D_2 are the calculated dissociative-attachment cross section using the semiempirical β_0 (Fig. 4) deduced from the (e, H_2) system.

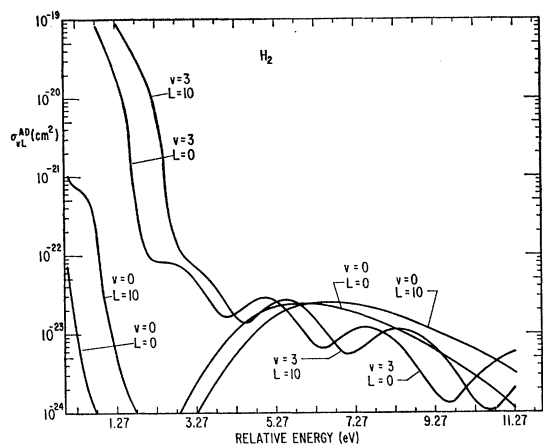


FIG. 7. The cross section for the production of H_2 in four depicted sets of rotational and vibrational states in associative detachment.

obtained are given in Figs. 3 and 4 for the $g \rightarrow u$ and $g \rightarrow g$ cases, respectively. It is seen that $\beta_1^{(u)}$ is, as expected, two orders of magnitude larger than $\beta_0^{(g)}$ and that they do not join smoothly to each other. This is because they are coming from different modes of interaction.

Having obtained the β 's, the reduced cross section for dissociative attachment for HD and D_2 can be easily obtained as byproducts since the β 's are practically mass-independent. They are plotted in Figs. 5 and 6 together with the H_2 system. For the $g \rightarrow u$ dissociative attachment (Fig. 5), the cross sections have vertical onsets. Such vertical onsets are expected since the ${}^2\Sigma_u^+H_2^-$ state has its well in the Franck-Condon region of the ${}^1\Sigma_g^+H_2$ state so that the lower portion (in the energy sense) of the temporarily formed H_2^- would be unable to dissociate. We note again that due to the fact that Γ_g is approximated by a phenomenological potential and that $\beta_0^{(g)}$ is determined from the (e, H_2) system without the dip at around 10 eV as measured

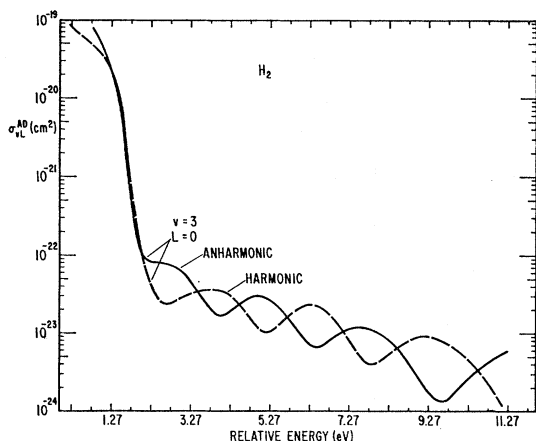


FIG. 8. The effect of anharmonicity in the vibrational motion of H_2 on associative detachment based on the Morse potential approximation.

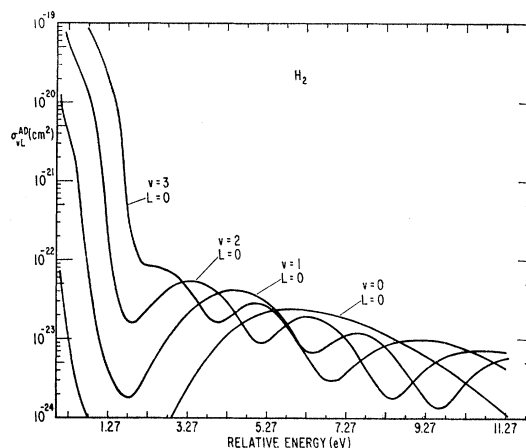


FIG. 9. The cross section for the production of vibrationally excited H_2 molecules in associative detachment.

by Rapp *et al.*,⁷ the reduced dissociative-attachment cross sections for the hydrogen isotopes deduced from the semiempirical β 's are also smooth without the dip.

Utilizing the semiempirical β 's the cross section for associative detachment for H and H^- is then calculated within the same approximations. The results are presented here in graphic form in Figs. 7–11.

From the consideration of the nuclear overlap integral we expect at low collision energy that electron detachment would be likely to take place at large internuclear separation, provided the interaction is complex there. As a consequence, higher vibrational states of the residual molecule are more likely to be populated than the lower states, which would give rise to an inverted population. The amplitude of electron detachment depends of course on the magnitude of the imaginary part of the interaction potential. This is a typical case for the (H, H^-) system, if H and H^- approach each other along the ungerade mode of interactions provided by the ${}^2\Sigma_u^+$ state of H_2^- at low energy. Since the ${}^2\Sigma_u^+$ state is attractive, H and H^- will be attracted towards

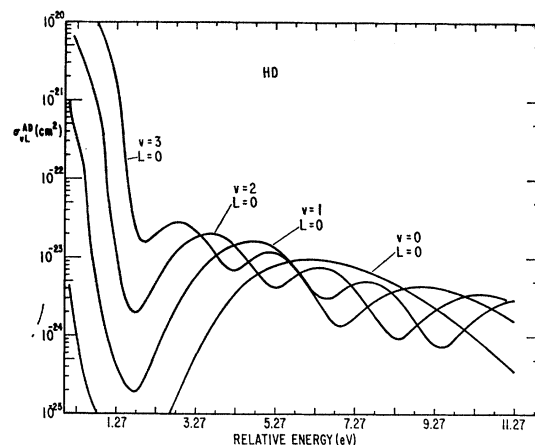


FIG. 10. The cross section for the production of vibrationally excited HD molecules in associative detachment.

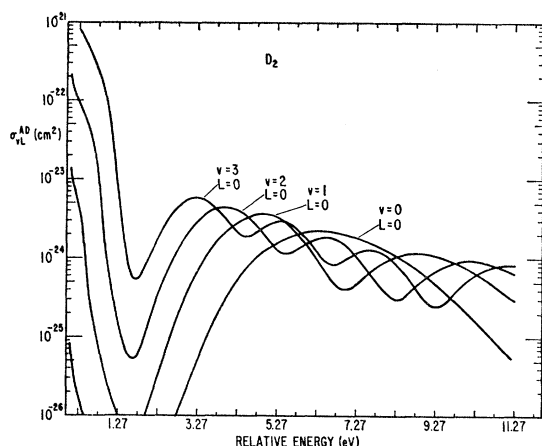


FIG. 11. The cross section for the production of vibrationally excited D_2 molecules in associative detachment.

each other as they approach the complex interaction region. A large associative-detachment cross section for the production of an excited H_2 molecule is then expected at low energy, say, less than a few electron volts.

As the colliding energy becomes higher, the damping nuclear wave function ξ oscillates more rapidly and the overlap integral with the vibrational wave function of the residual molecule will then cut down the cross section for associative detachment. However, if the classical turning point of ξ lies within the Franck-Condon region of the residual molecule, the nuclear overlap integral may still be appreciable due to the pile up of the amplitude of ξ at the turning point. Since the vibrational wave function of the residual molecule may also oscillate, we then expect the cross section to oscillate accordingly as a function of energy, which results from the movement of the classical turning point with respect to the energy along the interaction potential. This is the situation for the (H, H^-) system if H and H^- approach each other along the gerade mode of interaction. Since, in this mode, the interaction is repulsive, H and H^- cannot, at low energy, approach each other sufficiently close to enter the complex interaction region for electron emission. At higher energy H and H^- can, however, penetrate into the complex interaction region. In this case, the damping nuclear wave function oscillates more rapidly so that the overlap integral is appreciable only at the classical turning points.

In Fig. 7, the partial cross sections are plotted for four depicted sets of vibrational and rotational states (vL) of H_2 to demonstrate the foregoing discussed effects. It is seen that the cross section for the production of (3,10) states of H_2 is much larger than that for the (0,0) state at low energy due to the ungerade mode of interaction. The increase of the cross section with respect to the rotational states is, however, much smaller than it is with respect to the vibrational states. As expected, the cross section drops rapidly as energy increases. At higher energy, say, $E > 3$ eV, the contribu-

tion due to the gerade mode of interaction becomes significant. Since the contribution to the nuclear overlap integrals comes largely from the turning point along the interaction, we observed the oscillating behavior of the cross section corresponding to the oscillation of the vibrational wave function.

In this calculation the vibrational wave function of the H_2 molecule is taken to be the Morse anharmonic wave function. A comparison of this approximation with the harmonic-oscillator wave-function approximation is given in Fig. 8. It is seen that the anharmonic effect is of significance even for relatively low vibrational states. For higher vibrational states, the effect would be of course more pronounced. We have neglected the coupling between rotational and vibrational motions for the H_2 molecule. This coupling is believed to be small.

The isotope effect in associative detachment is illustrated in Figs. 9–11 for H_2 , HD, and D_2 , respectively. It is seen that the partial cross-section decreases with the increase in mass. In these figures a comparison of the cross section for the production of the residual molecule in various vibrational states is also given for the ground rotational states. In all these results it is seen that the partial cross section rises rapidly as the incident energy becomes small. Consequently, the dominant contribution to the large rate coefficient comes from the cross section at very low relative energies of H and H^- .

No experimental measurement of the associative-detachment cross section has been reported in the literature for comparison. Most measurements concerning electron detachment are designed for the measurement of the rate coefficient.^{14,15} From the rate coefficient, it is, however, not a simple matter to deduce the total cross section and to isolate the portion for associative detachment. The total associative-detachment cross section can be calculated by a sum over all the partial cross sections.

For sufficiently low energy, the total associative-detachment cross section can be more easily obtained since there is a threshold for the collisional detachment channel. It is obvious that below the threshold energy (0.755 eV), the entire electron emission amplitude arises directly from the associative-detachment channel and the residual molecule would not have sufficient energy to dissociate. If one is not interested in the final vibrational and rotational states of the residual molecule, the total cross section for associative detachment can be obtained from Eqs. (1.4) and (1.6). At still lower energies, say, below about 0.255 eV, the gerade mode of interaction ceases to give rise to any amplitude for associative detachment, simply because H and H^- being at such low energy cannot get close enough under the

¹⁴ A. L. Schmalzshopf, F. C. Fehsenfeld, and E. E. Ferguson, *Astrophys. J.* **148**, 155 (1967).

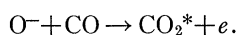
¹⁵ J. L. Pack and A. V. Phelps, *J. Chem. Phys.* **44**, 1870 (1966); **45**, 4316 (1966).

repulsive potential to be in the complex-potential region for electron emission. Thus at such a low-energy region only the ungerade mode of interaction is of importance.

IV. CONCLUSIONS

We have examined the energy dependence of the partial cross section for the production of residual H_2 molecules in various vibrational and rotational states in associative detachment. The gross features of the calculated cross section can be understood based on the present theory of associative detachment.^{4,16} The cross section becomes very large only at extremely low relative energy of H and H^- . Unfortunately, there are no detailed experimental measurements reported in the literature for comparison. A wealth of information could be obtained experimentally by measuring the energy and angular distributions of the detached electron. At relative energies of H and H^- below the detachment potential of the negative H^- ions, detailed information concerning the distribution of the residual molecular states can be simply deduced by measuring the electron energy distribution. The contribution to associative detachment from the ungerade and gerade modes of interaction can, with the help of the selection rules,⁹ be resolved by measuring the angular distribution of the detached electron.

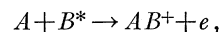
One of the important features in associative detachment is the production of "hot" residual molecules, even at low temperatures. From the present calculations it is observed that higher vibrational and rotational states are more likely to be populated than the lower ones. Thus, associative detachment provides a mechanism for generating an inverted population, a phenomenon of great practical interest in connection with laser construction. An interesting system to investigate is



Here the residual CO_2 molecule may participate in three different modes of vibration. Crude geometrical considerations seem to indicate that the process of associative detachment is more likely to populate the asymmetrical mode of vibration than the other two

¹⁶ Since the work was completed a paper by A. Herzenberg has been published [Phys. Rev. **160**, 80 (1967)] which contains similar theoretical results as those in Ref. 4. Also, it contains a qualitative discussion on the behavior of the associative-detachment cross section which is consistent with the results presented in the present paper. However, no detailed calculations were reported there.

remaining (symmetrical) modes of vibration in CO_2 . The very high vibrational states of CO_2 (or H_2) lying above the asymptotic limit of O^- and CO (or H and H^-) are, however, not accessible to the associative detachment due to the energy limitation. Also of interest is the process of associative ionization,



involving a metastable atom or molecule B^* .

APPENDIX: APPARENT THRESHOLD BEHAVIOR

It perhaps is worthwhile to mention that for processes with a threshold such as dissociative attachment, the measured apparent threshold behavior appears to rise less rapidly than the actual threshold behavior under the simple influence of the experimental beam width. This is because a constant normalization for the beam distribution is usually used in the experiment. This constant normalization is, however, not the natural one to use near the threshold as shown in Fig. 12(a), where

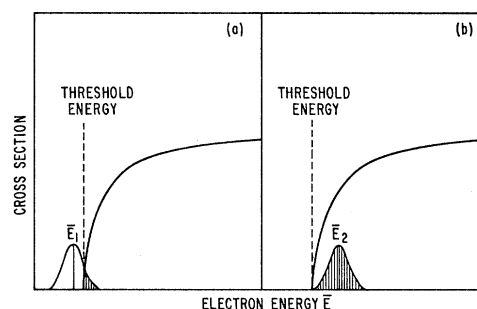


FIG. 12. Schematic diagram of the beam spread in connection with the threshold behavior.

only a shaded portion of the beam distribution may contribute to the process. By dividing the scattered current by the complete area of the beam width one would make the threshold behavior proportionally smaller than it should be. As the mean energy E of the beam moves away from the threshold to the higher-energy side, the normalization becomes a constant as soon as the spread of the beam width does not significantly overlap with the threshold energy as shown in Fig. 12(b). Since the threshold energy of the process under measurement is usually unknown prior to the measurement, a constant normalization is therefore usually used. Caution should then be exercised in examining the threshold behavior.